BMC Cardiovascular Disorders

RESEARCH Open Access

Aortic arch anatomical differences in male type B aortic dissection patients vs. healthy male individuals

Gaoxiang Wei[1,2*]

Abstract

Background Understanding the distinct anatomical differences between patients with type B aortic dissection (TBAD) and control patients (CPs) can enhance our knowledge of normal and pathological aortic dimensions. This study aimed to deepen our knowledge of these dimensions by measuring and comparing the anatomical indices of the aortic arch in male patients with TBAD and non-TBAD male patients.

Methods In this cross-sectional observational study, 62 TBAD patients (TBADPs) and 43 CPs were assessed. Using a fit centerline approach, we identified three pivotal anatomical landmarks: Point A, Point B, and Point C. These landmarks represented intersections of the aortic arch with the brachiocephalic trunk, left common carotid artery, and left subclavian artery, respectively. These points defined Zones 1, 2, and 3, which collectively span the entire proximal aorta from the proximal end of the aortic valve to Point C. Our analyses compared key anatomical indices such as diameter of the circumscribed circle (Dcirc), ellipticity, curvature, tortuosity between TBADP and CP at critical points and regions.

Results TBADPs showed a more circular cross-sectional shape at Points A, B and C, as indicated by reduced values of Dcirc_A ($P=0.031$), ellipticity_A ($P=0.034$) and ellipticity_B ($P=0.048$), together with a significant decrease in Dcirc_C ($P=0.015$) and ellipticity_C ($P=0.007$). The aortic arch in TBADPs showed enhanced tortuosity in Zone 1 ($p=0.002$) and extended elongation in Zone 3 ($p=0.001$).

Conclusions The study found that the aortic arch in male TBAD patients is more circular near its primary branches, has greater tortuosity in Zone 1, and is longer in Zone 3 compared to male control patients.

Keywords Aortic Dissection, Type B, Anatomy, Aorta, Cross-sectional shape

*Correspondence:
Gaoxiang Wei
gzsweigaoxiang@outlook.com
[1]Department of Thoracic Surgery, Shunde Hospital of Southern Medical University (The First People's Hospital of Shunde), Foshan, Guangdong 528308, China
[2]Department of Cardiovascular Medicine, Guangzhou First People's Hospital, School of Medicine, South China University of Technology, Guangzhou, Guangdong 510180, China

Background

Thoracic endovascular aortic repair (TEVAR) is a pivotal treatment strategy for type B aortic dissection (TBAD) [1]. Given that intramural hematomas or tears frequently occur near the left subclavian artery and considering the stringent requirements for the length of the anchoring zone in current stent-graft designs, endovascular treatments for TBAD currently face challenges in both anchoring within the aortic arch and in reconstructing its major branches [2, 3]. While interventions involving the descending aorta can often be straightforward, the unique and intricate anatomy of the aortic arch brings forth multifaceted challenges. Preoperative aortic arch excessive aortic arch angulation, defined as the angle between the tangent lines at the starting point of the brachiocephalic trunk coverage segment and at the endpoint of the left subclavian artery coverage segment on the aortic centerline, can cause complications, leading to insufficient adherence between the stent and the aortic arch tissue, especially along the inner side where the curvature is greater. This inadequate adherence frequently manifests as the 'bird-beak sign', a disconcerting indicator associated with complications such as endoleaks, stent migration, and long-term technical failure [4]. In addition to the challenges posed by the curvature of the arch, the varying vascular length, regional tortuosity, and geometric parameters at specific branch points further complicate stent placement and performance [5, 6]. For instance, the lengths of different zones within the arch might influence the stress and strain experienced by stents. Moreover, regional tortuosity might result in uneven force distribution across the stent. Furthermore, geometric parameters at crucial aortic branch points, such as the diameters of inscribed and circumscribed circles and the ellipticity, might have pronounced implications for stent design and adherence [7]. Despite significant advancements in stent technology, persistent issues with stent adherence in TBAD patients (TBADPs) post-TEVAR underline the need for a more refined understanding of the geometry of the aortic arch. By utilizing postprocessing techniques from computed tomography angiography (CTA) imaging, our study further investigates this area of research. By employing centerline extraction and related parameter measurement techniques, we aimed to perform a meticulous evaluation of the anatomical and hydraulic parameters of the aortic arch in both control patients (CPs) and TBADPs. The overarching goal is to furnish pivotal geometric insights that can steer the evolution and optimization of intraluminal devices for TBAD, ensuring enhanced stent adherence and improved patient outcomes.

Methods

Data sources and selection criteria

This retrospective study enrolled a total of 62 patients who were diagnosed with TBAD at Guangzhou First People's Hospital between January 2020 and March 2023. The inclusion criteria stipulated that participants must possess complete CTA records. The exclusion criteria included connective tissue disorders, a history of aortic surgery, intramural hematoma or rupture involving the left subclavian artery, and displaying anatomical variations in the aortic arch, such as a "bovine arch." For the control group, a total of 43 male individuals from the CPs who underwent thoracic CTA examinations at Guangzhou First People's Hospital from January 2020 to March 2023 were selected. The control group underwent thoracic CTA primarily due to the clinical suspicion of cardiovascular diseases. Once cardiovascular diseases were ruled out by CTA, these patients were included in the control group for this study. The inclusion criteria required that the CTA scans encompass both the ascending aorta and the aortic arch. Exclusion criteria ruled out individuals with aortic dissection, aortic aneurysms, or other aortic-related diseases, as well as those with a history of aortic surgery, connective tissue disorders, or anatomical variations in the aortic arch, such as a "bovine arch."The scanning parameters were as follows: tube voltage of 100 kV, automatic tube current, contrast agent Iopromide at 370 mgI/ml, total contrast volume of 70 ml administered at 4 ml/s, slice thickness of 1 mm, and a pitch factor of 0.6.

Image postprocessing methodology

CTA images from all study participants were imported into the semiautomated postprocessing software Mimics (version 21.0, Belgium) in Digital Imaging and Communications in Medicine format. For the processing workflow, the initial steps involved the precise segmentation of the aortic arch and its major branches, including the brachiocephalic trunk, left common carotid artery, and left subclavian artery. This segmentation started from the proximal plane of the aortic valve and extended distally.

The segmentation process is as follows: First, a threshold range of 226 to 3071 is set, and the hole-filling function is enabled. The boundaries are adjusted with the lower boundary at the heart's inferior edge, lateral boundaries at the heart's lateral margins, the anterior boundary at the heart's anterior margin, the posterior boundary at the descending aorta's posterior edge, and the upper boundary at the scan's topmost edge. A mask is generated based on these settings. Then, using the "split mask" tool, "Region A" is manually marked to include the aortic arch and its major branches, while "Region B" is manually marked to exclude non-target areas like the atria, ventricles, pulmonary vessels, and bony structures.

Through this process, the aortic arch is fully segmented from the thoracic aorta, extending from the aortic valve to the inferior edge of the heart, while the major branch vessels of the aortic arch are also separated. Subsequently, a three-dimensional model of the aortic arch and its branches was constructed based on the segmentation results. The segmentation of the aorta in our study includes all enhanced regions, encompassing both the true lumen and the false lumen, as well as the septum between the true and false lumen, excluding any thrombus.

We utilized the "Fit Centerline" tool in to extract the centerline from reconstructed 3D models. The specific method is as follows: first, the smooth factor was set to 0.5, and the parameters for resolving resolution and distance between control points were set to automatic mode. Under these settings, the software automatically detects the geometric details of the model, generates the centerline, and identifies the intersection points between the centerline of the aortic arch and the main branch centerlines, which are then smoothed using a Fourier smoothing algorithm. The geometric centerline was derived to further analyze the structure and morphology of the aortic arch and its primary branches (Fig. 1), All the relevant parameters of points and curve segments were derived using the "Export Centerline Properties" tool within the Mimics software. The method of centerline extraction and parameter derivation has been applied in previous studies [8].

Location of anatomical landmarks

A fit centerline approach was employed to identify three pivotal anatomical landmarks: Point A (the intersection between the brachiocephalic trunk centerline and the aortic arch centerline), Point B (the intersection between the left common carotid artery centerline and the aortic arch centerline), and Point C (the intersection between the left subclavian artery centerline and the aortic arch centerline). Using these landmarks, sections from the proximal end of the aortic valve to Point A and segments AB and BC were categorized as Zone 1, Zone 2, and Zone 3, respectively. Zones 1–3 collectively represent the entire proximal aorta, extending from the proximal end of the aortic valve to the intersection at Point C (Fig. 1).

Measurement of anatomical indices

Vascular lengths in different regions: The lengths of Zones 1, 2, and 3, as well as the aggregate length of Zones 1–3, were calculated. Tortuosity in different vascular regions: Precise measurements of tortuosity were conducted for Zones 1, 2, and 3 and for the composite Zone 1–3. Tortuosity is defined as T=1–(straight line distance/distance along the centerline). This definition has been consistently used in previous studies [8]. Geometrical parameters at the aortic arch branch points: For the key landmarks Points A, B, and C and their corresponding aortic arch regions, the following geometric parameters were computed: diameter of the best-fit circle (D_{fit}), diameter of the inscribed circle (D_{in}), diameter of the circumscribed circle (D_{circ}), circumference, cross-sectional area (CA), curvature, and ellipticity (see supplementary materials for detailed information). The software does

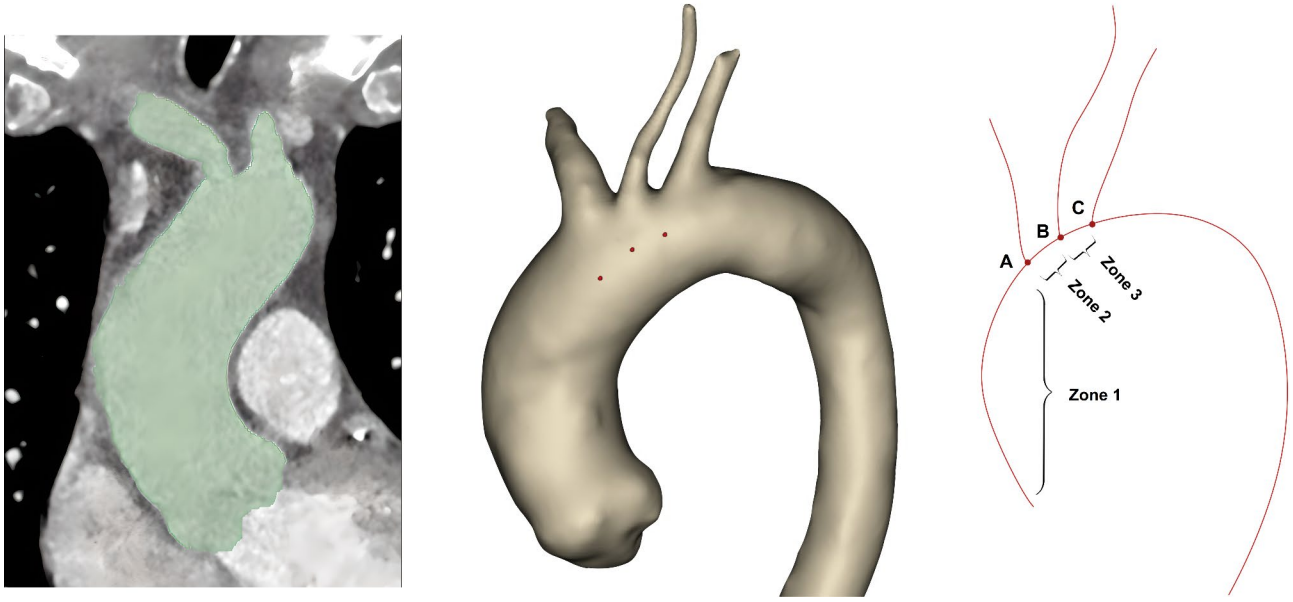

Fig. 1 Extraction process of the aortic arch and its major branch centerlines

not disclose the specific algorithms used for best-fit circle and curvature parameter calculations, the calculation principles for other parameters are provided in Fig. 2.

Measurement of hydraulic parameters

Hydraulic diameter (HD): This parameter serves as a critical parameter for characterizing fluid flow properties in noncircular conduits and is commonly used in the study of fluid mechanics and thermodynamics within pipes [9, 10]. The diameter of a circular pipe is equivalent to its hydraulic diameter. A larger HD generally corresponds to higher flow efficiency, while a smaller HD may lead to greater flow resistance and energy loss. Hydraulic ratio (HR): HR=HD / Dcirc, when HR is close to 1 in non-circular pipes, it indicates that the shape has flow characteristics similar to a circular pipe. (see the supplementary materials for detailed information). The calculation principles for HD and HR are provided in Fig. 2.

Statistical analysis

All the statistical calculations in this study were performed using Python 3, and a *P*value less than 0.05 was considered to indicate statistical significance.

Comparison of clinical data

We statistically analyzed clinical data, including age, history of hypertension, height, weight and body mass index (BMI), in two different groups, the CP and TBADP groups. The Shapiro–Wilk test confirmed the normal distribution of the continuous variables, which are presented as mean±standard (x±s). For comparisons between groups, the independent samples t-test was used for continuous variables. Categorical variables are presented as proportions and were compared using the chi−squared test.

Comparison of the anatomical and hydraulic parameters of the aortic arch

An independent-samples t-test was conducted to directly compare the anatomical and hydraulic parameters of the aortic arch between the CP and TBADP groups. Subsequently, a multivariate linear regression analysis was used to compare the anatomical and hydraulic parameters of the aortic arch between the CP and TBADP groups. This analysis included covariates such as age, history of hypertension, height, weight and BMI, controlling for demographic and health-related factors. The regression models provided detailed insights, including regression coefficients, t-statistics and *p* values.

Results

Clinical data comparison

In our study, we observed statistically significant differences in clinical characteristics between the TBADP and CP groups. The mean age of the TBADP group was 53.37±12.07 years, ranging from 29 to 78 years, which was significantly younger than that of the CP group. The mean age of the CP group was 63.00±14.77 years, with a broader age range from 17 to 94 years ($p<0.001$). A striking 95.2% of the TBADP group had a history of hypertension, which is a considerably greater proportion than the 39.5% observed in the CP group ($p<0.001$). Furthermore, the individuals in the TBADP group were taller on average (168.19±5.36 cm vs. 164.70±6.22 cm, $p=0.003$), were heavier (74.94±13.09 kg vs. 62.07±13.39 kg, $p<0.001$), and had a greater body mass index (BMI) (26.43±4.07 vs.

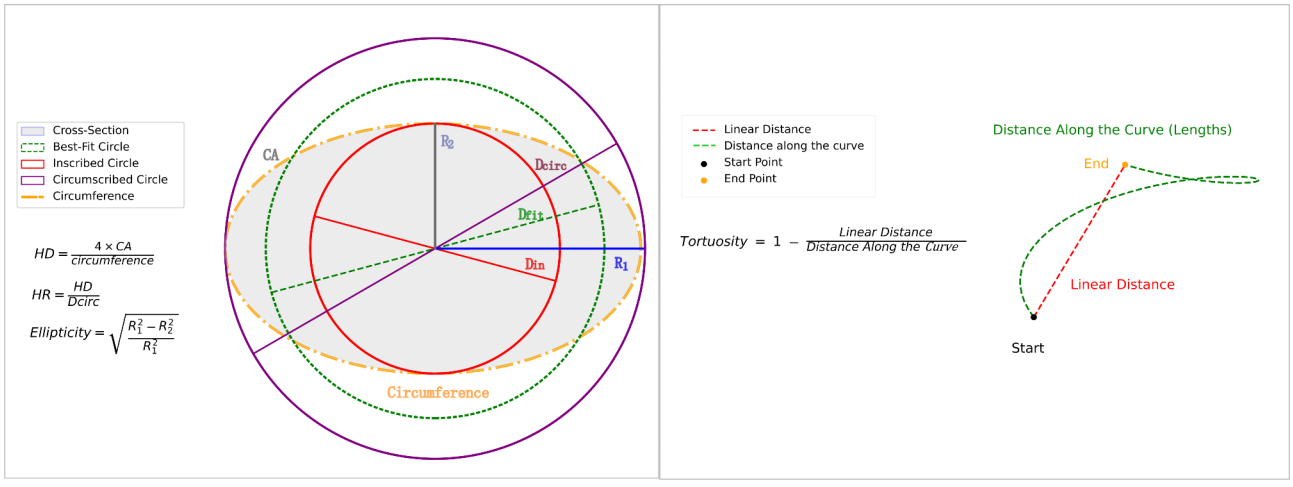

Fig. 2 Calculation Principles for Vascular Parameters
Dfit: diameter of the best-fit circle; Din: diameter of the inscribed circle; Dcirc: diameter of the circumscribed circle; HD: hydraulic diameter; HR: hydraulic ratio; CA: cross-sectional area

22.79±4.16, $p<0.001$) than individuals in the CP group (Table 1).

Comparison of aortic arch anatomical indicators

Anatomical and hydraulic parameters at Point A

At Point A, where the centerline of the brachiocephalic artery intersects with the centerline of the aortic arch, we observed significant differences between male TBADPs and male CPs (see Supplementary Tables 2–10 for covariate details in the model; see Supplementary Fig. 1 for direct parameter comparisons). Specifically, in the male CP group, Dcirc_A was significantly higher than in the male TBADP group (regression coefficient=10.39, 95% CI [0.96, 19.81], $p=0.031$), indicating that after adjusting for age, hypertension, height, weight, and BMI, this parameter was 10.39 mm higher in the CP group (Fig. 3). Additionally, ellipticity_A was also significantly higher in the CP group (regression coefficient=0.10, 95% CI [0.01, 0.19], $p=0.034$), showing an increase of 0.10 units after similar adjustments.

Anatomical and hydraulic parameters at Point B

At Point B, the critical intersection where the left common carotid artery meets the centerline of the aortic arch, a significant difference in ellipticity_B was observed between male TBADPs and male CPs (see Supplementary Tables 11–19 for covariate details in the model; see Supplementary Fig. 2 for direct parameter comparisons). Ellipticity_B was significantly higher in the CP group compared to the TBADP group, with a regression coefficient of 0.11 (95% CI [0.00, 0.22], $p=0.048$), indicating that after controlling for confounding factors, the CP group exhibited a 0.11 unit increase in ellipticity_B relative to the TBADP group (Fig. 3).

Anatomical and hydraulic parameters at Point C

At Point C, where the centerline of the subclavian artery intersects with the centerline of the aortic arch, we also observed significant differences in multiple parameters between the TBADP and CP groups (see Supplementary Tables 20–28 for covariate details in the model; see Supplementary Fig. 3 for direct parameter comparisons). Dcirc_C was significantly higher in the CP group compared to the TBADP group, with a regression coefficient of 12.93 (95% CI [2.52, 23.34], $p=0.015$), indicating that after adjusting for confounding factors, this parameter was 12.93 mm greater in the CP group. Conversely, HD_C and HR_C were both significantly lower in the CP group compared to the TBADP group, with regression coefficients of -1.97 (95% CI [-3.84, -0.09], $p=0.040$) and −0.15 (95% CI [-0.24, -0.05], $p=0.003$), respectively. This suggests that after similar adjustments, the CP group exhibited decreases of 1.97 mm and 0.15 units in HD_C and HR_C, respectively. Additionally, Ellipticity_C was significantly higher in the CP group, with a regression coefficient of 0.13 (95% CI [0.03, 0.22], $p=0.007$), showing an increase of 0.13 units after adjusting for confounding factors.(Fig. 3).

Comparative analysis of aortic arch anatomy and tortuosity between healthy individuals and patients with aortic dissection

Upon comparing the TBADP group with the CP group, we discerned notable differences in both the lengths and tortuosity of specific aortic zones (see Supplementary Tables 29–36 for covariate details in the model; see Supplementary Fig. 4 for direct parameter comparisons). Based on the regression analysis, Zone3_length was significantly shorter in the CP group compared to the TBADP group, with a regression coefficient of -7.52 (95% CI [-12.91, -2.13], $p=0.007$), indicating that after adjusting for confounding factors, the Zone3_length was 7.52 mm shorter in the CP group. Similarly, Zone1-3_length was significantly shorter in the CP group, with a regression coefficient of -13.11 (95% CI [-22.36, -3.86], $p=0.006$), suggesting a 13.11 mm decrease in Zone1-3_length in the CP group after adjustments. Additionally, Zone1_Tortuosity was significantly lower in the CP group compared to the TBADP group, with a regression coefficient of -0.04 (95% CI [-0.07, -0.02], $p=0.002$), indicating a decrease of 0.04 units in Zone1_Tortuosity after adjustments. Lastly, Zone1-3_Tortuosity was also significantly lower in the CP group, with a regression coefficient of -0.05 (95% CI [-0.08, -0.02], $p=0.001$), reflecting a 0.05 unit decrease in tortuosity in the CP group after controlling for other factors (Fig. 4).

Table 1 Comparison of clinical characteristics between TBADPs and CPs

Variable	CP	TBADP	t/χ2	*P*
Age (x±s)	63.00±14.77	53.37±12.07	3.67	0.001
Height (x±s)	164.70±6.22	168.19±5.36	-3.07	0.003
Weight (x±s)	62.07±13.39	74.94±13.09	-4.91	0.001
BMI (x±s)	22.79±4.16	26.43±4.07	-4.47	0.001
Hypertension (n, %)			36.57	0.001
No	17 (39.53)	59 (95.16)		
Yes	26 (60.47)	3 (4.84)		

TBADP: Type B aortic dissection patient; CP: Control patient; x±s: Mean±standard

Discussion

TEVAR is currently the first-line therapeutic option for managing complicated TBAD. However, a healthy proximal landing zone is the premise of the approach and the determinant of its outcomes [11, 12]. Intentional coverage of the left subclavian artery to extend the landing zone is associated with a high risk of upper extremity ischemia and posterior circulation stroke [13]. Regardless

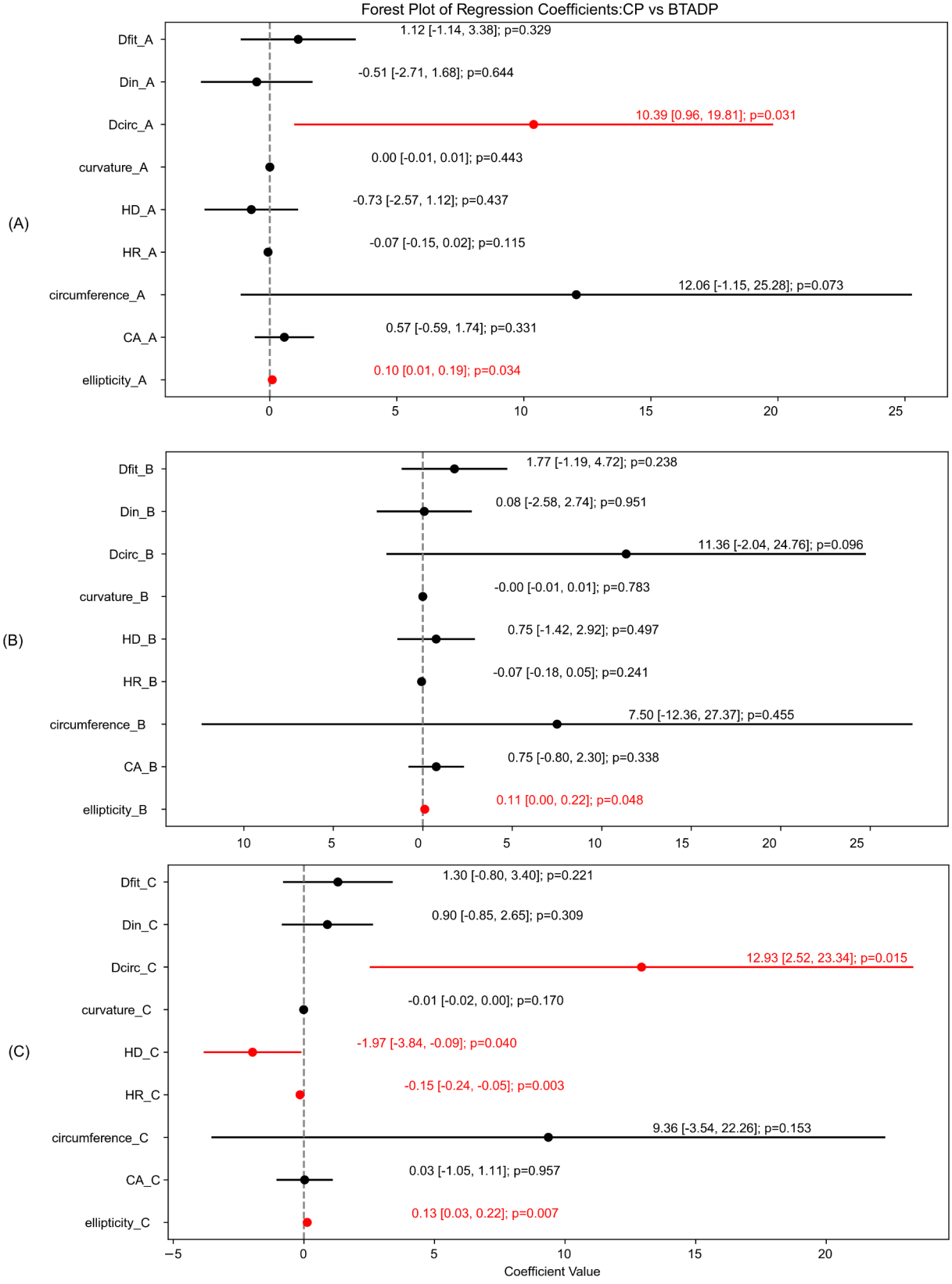

Fig. 3 Forest plot of regression coefficients comparing parameters between TBADPs and CPs. The TBADP group is used as the reference group, with positive coefficients indicating higher values in CPs relative to TBADPs. (**A**) Point A; (**B**) Point B; (**C**) Point C
D_{fit}: diameter of the best-fit circle; D_{in}: diameter of the inscribed circle; D_{circ}: diameter of the circumscribed circle; HD: hydraulic diameter; HR: hydraulic ratio; CA: cross-sectional area; TBADP: type B aortic dissection patient; CP: control patient

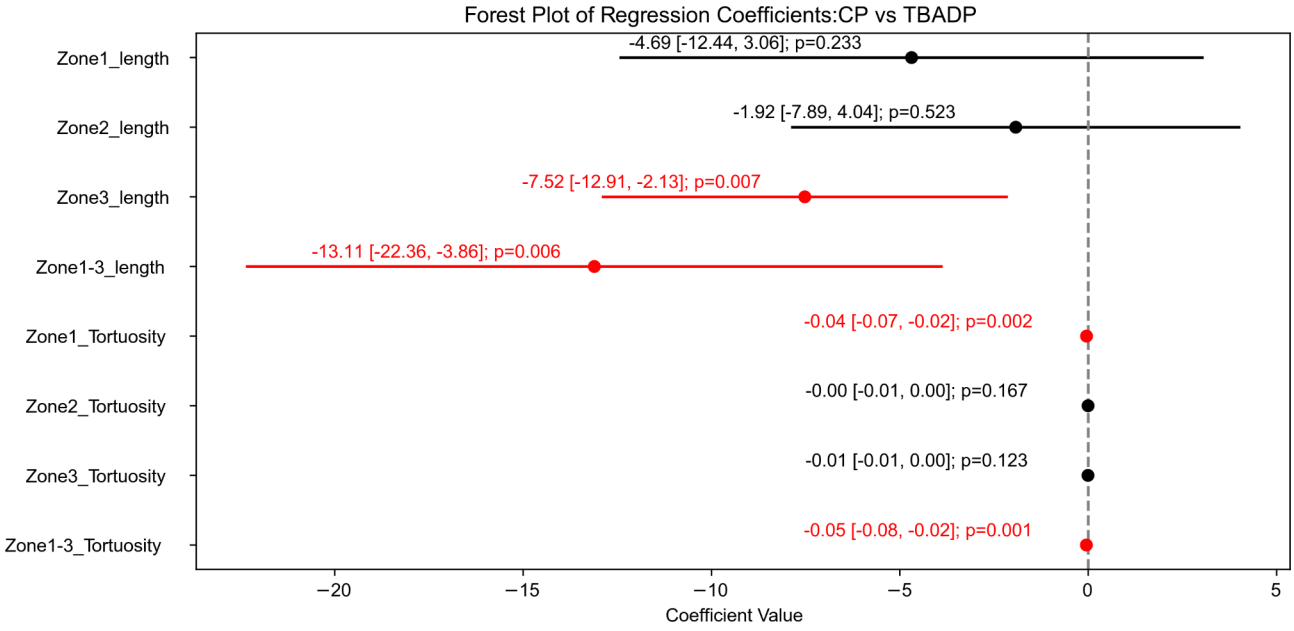

Fig. 4 Forest plot of regression coefficients comparing zone-related parameters between TBADPs and CPs. The TBADP group is used as the reference group, with positive coefficients indicating higher values in CPs relative to TBADPs
TBADP: Type B aortic dissection patient; CP: Control patient

of the choice between parallel stent technology, fenestration technique, or endovascular grafting methods for the reconstruction of supra-arch branches, the intimate anchoring and apposition of the main stent in the curved arch region remain pivotal for the success of TEVAR and favorable long-term arterial remodeling [14–16]. Clearly, defining the curvature of the aortic arch and its associated geometric parameters is crucial for enhancing the apposition performance of stents in the curved aortic arch [17]. In this study, we explored the anatomical and hydraulic parameters of TBADPs using the centerline and anatomical landmarks on the centerline.

At Point A, the D_{circ}_A (p=0.031) and ellipticity_A (p=0.034) of TBADPs were significantly lower than those of CPs. This observation suggests that the cross-sectional shape of the aortic arch in TBADPs at Point A tends to be more regular and circular. At Point B, the ellipticity_B (p=0.048) of TBADPs was significantly lower than that of CPs. The vascular shape tends to be more circular at this point, which is consistent with the observation at Point A. At Point C, the D_{circ}_C (p=0.015) and ellipticity_C (p=0.007) of TBADPs were significantly lower than those of CPs. This finding is similar to the observation at Point A. These observations suggest that compared to that of male CPs, the aortic arch of male TBADPs near its primary branches tends to be more circular. At Point C, the HR_C (p=0.003) and HD_C (p=0.040) values in the aortas of TBADPs were greater than those in CPs. This elevation could be related to increased resistance and pressure at Point C due to the intramural hematoma being located distally.

Aditya S Shirali et al. [18] found that the enlargement of the ascending aorta and aortic arch, coupled with heightened aortic tortuosity, indicates an aortopathy that increases the likelihood of TBAD. In this study, TBADPs exhibited a more curved aortic arch in Zone 1 (p=0.002) and Zones 1–3 (p=0.001) than in CPs. M Alban Redheuil et al. [19] found that there was a significant positive correlation between the length of the aorta and age. Our study yielded similar results, indicating that an increase in age is associated with an increase in the lengths of Zone 1 (P=0.013) and Zones 1–3 (P=0.005) (Supplementary Tables 29 and 32). Lescan et al. [20] discovered that aortic arch elongation is associated with the development of TBAD. We observed that the lengths of Zone 3 (p=0.007) and Zones 1–3 (p=0.006) in TBADPs were significantly greater than those in CPs. TBADPs displayed greater distances between the intersections of the left common carotid artery and the left subclavian artery on the aortic arch.

Current stents used for treating TBAD have evolved from designs originally intended for thoracic aortic aneurysms [21]. Importantly, various aortic diseases present different anatomical configurations of the arch [22]. Therefore, designing stents that specifically account for the unique anatomical characteristics of the aortic arch in TBADP patients may help improve surgical safety. In this study, we found that although the ellipticity_C at point C in TBADP is smaller compared to CP and closer

to a circular shape, the average ellipticity value is 0.59 (see Supplementary Fig. 3). This suggests that the arterial cross-section may still possess a non-circular shape. Therefore, the design of covered stents near point C should consider the possibility that the stent material and structure need to accommodate this non-circular geometry to potentially reduce localized stress concentration. The study also suggests that Zone 3 in TBADP may experience elongation, which could possibly lead to changes in the opening position of branch arteries. Consequently, it may be necessary to consider designing and selecting chimney grafts according to the patient's specific anatomical structure to ensure that the stent can adequately adapt to the elongated Zone 3 area and maintain its functionality. Additionally, this study suggests that TBADP may exhibit greater curvature in Zones 1–3 compared to CP. This implies that the stent delivery system may need to possess sufficient flexibility to navigate smoothly through the curved arterial path, ensuring accurate positioning and stable deployment of the stent.

This study has several limitations. First, due to the small number of female TBADPs, only male patients were included for comparison with CPs. Second, given the limited sample size of this study, no separate analysis was conducted for different subtypes of TBAD.

Conclusions

In summary, compared to that of male CPs, the aortic arch of male TBADPs near its primary branches tends to be more circular. Additionally, the aortic arch of male TBADPs possesses greater tortuosity in Zone 1 and a greater length in Zone 3.

Abbreviations

BMI	Body Mass Index
CA	Cross-Sectional Area
CP	Control patient
CTA	Computed Tomography Angiography
Dcirc	Diameter of the Circumscribed Circle
Dfit	Diameter of the Best Fit Circle
Din	Diameter of the Inscribed Circle
HD	Hydraulic Diameter
HR	Hydraulic Ratio
TBAD	Type B Aortic Dissection
TBADP	Type B Aortic Dissection Patient
TEVAR	Thoracic Endovascular Aortic Repair

Supplementary Information

The online version contains supplementary material available at https://doi.org/10.1186/s12872-024-04206-1.

Supplementary Material 1

Acknowledgements

We would like to express our deepest gratitude to the staff and colleagues in the Department of Radiology, Guangzhou First People's Hospital, for their help during the preparation of this work.

Author contributions

All the research was conducted by GW, and the manuscript was written by GW.

Funding

This research did not receive any grants from any funding agencies in the public, commercial, or not-for-profit sectors.

Data availability

The data that support the findings of this study are available from the corresponding author upon reasonable request.

Declarations

Ethics approval and consent to participate

All procedures performed in studies involving human participants were in accordance with the ethical standards of the institutional and/or national research committee and with the 1964 Helsinki Declaration and its later amendments or comparable ethical standards.

Research involving human participants and/or animals and informed consent

This retrospective study utilized anonymized existing data, informed consent was waived by the Ethics Committee of Guangzhou First People's Hospital. This study was approved by the Ethics Committee of Guangzhou First People's Hospital.

Consent of publication

Not applicable.

Competing interests

The authors declare no competing interests.

Received: 31 March 2024 / Accepted: 18 September 2024
Published online: 16 October 2024

References

1. Carrel T, Sundt TM 3rd, von Kodolitsch Y, Czerny M. Acute aortic dissection. Lancet. 2023;401(10378):773–88.
2. Kuo EC, Veranyan N, Johnson CE, Weaver FA, Ham SW, Rowe VL, Fleischman F, Bowdish M, Han SM. Impact of proximal seal zone length and intramural hematoma on clinical outcomes and aortic remodeling after thoracic endovascular aortic repair for aortic dissections. J Vasc Surg. 2019;69(4):987–95.
3. Zhang T, Jiang W, Lu H, Liu J. Thoracic endovascular aortic repair combined with assistant techniques and devices for the treatment of acute complicated stanford type B aortic dissections involving aortic arch. Ann Vasc Surg. 2016;32:88–97.
4. Cao L, Ge Y, He Y, Wang X, Rong D, Lu W, Liu X, Guo W. Association between aortic arch angulation and bird-beak configuration after thoracic aortic stent graft repair of type B aortic dissection. Interact Cardiovasc Thorac Surg. 2020;31(5):688–96.
5. Voskresensky I, Scali ST, Feezor RJ, Fatima J, Giles KA, Tricarico R, Berceli SA, Beck AW. Outcomes of thoracic endovascular aortic repair using aortic arch chimney stents in high-risk patients. J Vasc Surg. 2017;66(1):9–e2023.
6. Kan X, Ma T, Dong Z, Xu XY. Patient-specific virtual stent-graft deployment for type B aortic dissection: a pilot study of the impact of Stent-Graft length. Front Physiol. 2021;12:718140.
7. Plonek T, Zak M, Burzynska K, Rylski B, Gozdzik A, Kustrzycki W, Beyersdorf F, Jasinski M, Filipiak J. The combined impact of mechanical factors on the wall stress of the human ascending aorta - a finite elements study. BMC Cardiovasc Disord. 2017;17(1):297.
8. Mokin M, Waqas M, Chin F, Rai H, Senko J, Sparks A, Ducharme RW, Springer M, Borlongan CV, Levy EI, et al. Semi-automated measurement of vascular tortuosity and its implications for mechanical thrombectomy performance. Neuroradiology. 2021;63(3):381–9.
9. Chu L, Xu J, Li Z, Zhao X. Verification experiment of maximum hydraulic diameter in a novel three-dimensional asymmetric oscillating heat pipe. Case Stud Therm Eng. 2024;55:104175.

10. Chae M-S, Chung B-J. Influence of system buoyancy and hydraulic diameter on turbulent mixed convection in a rectangular duct. Int J Heat Mass Transf. 2021;176:121411.
11. Mesar T, Alie-Cusson FS, Rathore A, Dexter DJ, Stokes GK, Panneton JM. A more proximal landing zone is preferred for thoracic endovascular repair of acute type B aortic dissections. J Vasc Surg. 2022;75(1):38–46.
12. Erbel R, Aboyans V, Boileau C, Bossone E, Di Bartolomeo R, Eggebrecht H, Evangelista A, Falk V, Frank H, Gaemperli O, et al. Corrigendum to: 2014 ESC guidelines on the diagnosis and treatment of aortic diseases. Eur Heart J. 2015;36(41):2779.
13. Waterford SD, Chou D, Bombien R, Uzun I, Shah A, Khoynezhad A. Left subclavian arterial coverage and stroke during thoracic aortic endografting: a systematic review. Ann Thorac Surg. 2016;101(1):381–9.
14. Chang H, Wang Y, Liu B, Wang W, Li Y. Endovascular repair for acute type B aortic dissection with unfavorable proximal landing zone. Ann Thorac Surg. 2022;113(2):545–53.
15. Budtz-Lilly J, Støvring H. TEVAR time travel with Simpson. Eur J Vasc Endovasc Surg. 2023;65(6):861.
16. Zhu J, Dai X, Noiniyom P, Luo Y, Fan H, Feng Z, Zhang Y, Hu F. Fenestrated thoracic endovascular aortic repair using physician-modified stent grafts (PMSGs) in zone 0 and zone 1 for aortic arch diseases. Cardiovasc Intervent Radiol. 2019;42(1):19–27.
17. Meuli L, Zimmermann A. Proximal sealing length in TEVAR: dependent on aortic arch type? Eur J Vasc Endovasc Surg. 2021;62(3):431.
18. Shirali AS, Bischoff MS, Lin HM, Oyfe I, Lookstein R, Griepp RB, Di Luozzo G. Predicting the risk for acute type B aortic dissection in hypertensive patients using anatomic variables. JACC Cardiovasc Imaging. 2013;6(3):349–57.
19. Redheuil A, Yu WC, Mousseaux E, Harouni AA, Kachenoura N, Wu CO, Bluemke D, Lima JA. Age-related changes in aortic arch geometry: relationship with proximal aortic function and left ventricular mass and remodeling. J Am Coll Cardiol. 2011;58(12):1262–70.
20. Lescan M, Veseli K, Oikonomou A, Walker T, Lausberg H, Blumenstock G, Bamberg F, Schlensak C, Krüger T. Aortic elongation and Stanford B dissection: the Tübingen aortic pathoanatomy (TAIPAN) project. Eur J Vasc Endovasc Surg. 2017;54(2):164–9.
21. Ivancev K, Vogelzang R. A 35 year history of stent grafting, and how EVAR conquered the world. Eur J Vasc Endovasc Surg. 2020;59(5):685–94.
22. Alberta HB, Takayama T, Smits TC, Wendorff BB, Cambria RP, Farber MA, Jordan WD, Patel V, Azizzadeh A, Rovin JD, et al. Aortic arch morphology and aortic length in patients with dissection, traumatic, and aneurysmal disease. Eur J Vasc Endovasc Surg. 2015;50(6):754–60.

Publisher's note